Scattering of Electromagnetic Wave by Large Open-Ended Cavities with Surface Impedance Boundary Conditions

Masato Tadokoro† and Kohei Hongo††

† The Yokohama Rubber Company , 2-1 Oiwake, Hiratsuka City, 254-8601, Kanagawa,Japan
tado@mta.yrc.co.jp

†† Department of Information Science, Toho University, Miyama 2-2-1, Funabashi,274-8510, Japan
hongo@is.sci.toho-u.ac.jp

1. Introduction

An analysis of the electromagnetic (EM) plane wave scattering from open-ended waveguide cavity configuration is important task in radar cross section (RCS) prediction of complex targets. Many practically useful approaches have been developed to analyze this kind of problem, such as, waveguide modal analysis, shooting and bouncing rays, Gaussian beam shooting method, moment method with a connection scheme, iterative physical optics (IPO), progressive physical optics, and so on. The review and references of these methods can be found in many published papers. We refer here only [1] $\sim$ [3] for saving space. It was pointed out [1] that impedance walls can reduce the RCS of the cavities. Almost all the approaches mentioned above can apply to the general cavities with surface impedance, but the most numerical results are devoted to verify the validities of the proposed analytical methods and are restricted to the cavities of the perfect conductor. So it is the purpose of this paper to investigate quantitatively how impedance wall can act for reducing the RCS of the cavity by applying the IPO algorithm. The IPO is the method of solving the magnetic field integral equation (MFIE) by using the iteration. Thus it may be interpreted as the extension of the conventional PO to apply to the problem having the multiple reflection. The IPO is more approximate than a matrix solution of MFIE, but it is quite accurate for electrically large cavity and is much more efficient.

The boundary integral equation (BIE) is developed for the equivalent electric currents on the interior walls with surface impedance boundary conditions. This equation is solved by using the IPO algorithm given in [2]. In contrast to the case of the cavity of perfect conductor, BIE of the impedance cavity contains the second derivatives of Green's function in the integrands. How to treat this singular integrals is discussed in [3]. The singular integrals over rectangular region can be represented by a simple elementary functions. The monostatic RCS of the circular waveguide cavity with surface impedance interior walls is computed for various values of surface impedance and it is found that the impedance walls are effective for reducing the RCS of open-ended cavities.

2. Theory

Boundary integral equation for the equivalent electric currents on the interior walls of the cavity is given by

$$\begin{aligned}\mathbf{J}(\mathbf{r}_c) = 2\mathbf{n}\times\mathbf{H}^i(\mathbf{r}_c) + 2\mathbf{n}\times\oint_{S_c}\mathbf{J}(\mathbf{r}'_c)\times\nabla' G_0(\mathbf{r}_c,\mathbf{r}'_c)dS'_c \\ + j\frac{\zeta_s}{k}\int_S\left[k^2 G_0(\mathbf{r},\mathbf{r}'_c) + \nabla'\nabla' G_0(\mathbf{r}_c,\mathbf{r}'_c)\right]\cdot[\mathbf{n}\times\mathbf{J}(\mathbf{r}'_c)]dS'_c \end{aligned} \quad (1)$$

where $\oint_{S_c}$ denotes the principal value of the integral, $\mathbf{r}_c$ and $\mathbf{r}'_c$ are the displacement vectors of observation and source points, respectively, ζ_s is the normalized surface impedance of the interior walls, and boudary condition $\mathbf{M} = -\zeta_s Z_0(\mathbf{n}\times\mathbf{J})$ is used. $\mathbf{M} = \mathbf{E}\times\mathbf{n}$ is the equivalent magnetic surface current, $G_0(\mathbf{r}_c,\mathbf{r}'_c)$ is free-space Green's function, and $\mathbf{n}$ is the unit normal of the interior walls. The symbol ∇' means that the

differentiation operates on $\mathbf{r}'$. $\mathbf{H}^i$ is the magnetic field produced by the field on the cavity aperture. It is noted that the last term contains second derivatives of the Green's funciton and we evaluate them according to Miron's analysis [4]. Eq.(1) is solved iteratively using the IPO algorithm. Once the equivalent electric currents on the interior walls of the cavity are determined, the scattered field produced by the currents is evaluated by

$$\mathbf{E}^s(\mathbf{r}_P) = \frac{-jkZ_0}{4\pi R}\exp(-jkR)\int_{S_c}\{[\mathbf{J}_c(\mathbf{r}'_c) - \mathbf{i}_R\mathbf{i}_R\cdot\mathbf{J}(\mathbf{r}'_c)] + \zeta_s\mathbf{i}_R\times[\mathbf{n}\times\mathbf{J}_c(\mathbf{r}'_c)]\}\exp[jk\mathbf{r}'\cdot\mathbf{i}_r]dS'_c \qquad (2)$$

The monostatic radar cross section is computed from the relation

$$\begin{aligned}\sigma &= 4\pi R^2\frac{|E^s|^2}{|E^i|^2}\\ &= \frac{k^2Z_0^2}{4\pi}\left|\int_{S_c}\{J_u(\mathbf{r}'_c)[(\mathbf{i}_\theta\cdot\mathbf{i}_u) - \zeta_s(\mathbf{i}_v\cdot\mathbf{i}_\phi)] + J_v(\mathbf{r}'_c)[(\mathbf{i}_\theta\cdot\mathbf{i}_v) + \zeta_s(\mathbf{i}_u\cdot\mathbf{i}_\phi)]\}\exp[jk\Phi(\theta_0,\phi_0)]dS'_c\right|^2\\ &+ \frac{k^2Z_0^2}{4\pi}\left|\int_{S_c}\{J_u(\mathbf{r}'_c)[(\mathbf{i}_\phi\cdot\mathbf{i}_u) + \zeta_s(\mathbf{i}_v\cdot\mathbf{i}_\theta)] + J_v(\mathbf{r}'_c)[(\mathbf{i}_\phi\cdot\mathbf{i}_v) - \zeta_s(\mathbf{i}_u\cdot\mathbf{i}_\theta)]\}\exp[jk\Phi(\theta_0,\phi_0)]dS'_c\right|^2\\ \Phi(\theta_0,\phi_0) &= x'\sin\theta_0\cos\phi_0 + y'\sin\theta_0\sin\phi_0 + z'\cos\theta_0 \qquad (3)\end{aligned}$$

where (x', y, z') and (u, v) are the global and localized rectangular coordinates of the discretized meshes of the walls, respectively. The symbol (R, θ, ϕ) are the spherical coordinates of the observation point extrior to the cavity and $\mathbf{i}_\xi$ is the unit vector with the direction of increasing ξ.

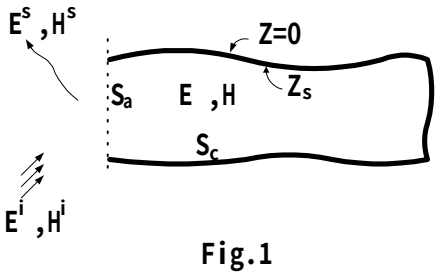

Fig.1

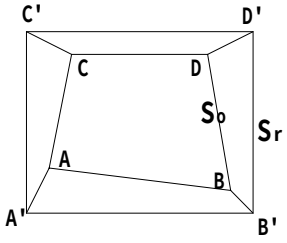

Fig.2

Fig.1 Cavity, **Fig.2 Four sided and rectangular meshes**

3. Numerical Results and Discussion

Interior walls of the cavity is divided into small four sided meshes. Global Cartesian coordinates of the nodes of the meshes are described $X(I, J)$, $Y(I, J)$, and $Z(I, J)$ with two kinds of indices I and J, and these data are stored in the memories of the computer. The center of each mesh is chosen to be the origin of the localized rectangular coordintes (u, v, w). The coordinates (u, v) are on the interior walls and w is normal to the walls. When the observation point is located inside the integral mesh, the original mesh S_o is changed to rectangular mesh S_r in order to perform the integral of the last term of eq.(1) analytically. The contributions from $S_o - S_r$ may be computed numerically since the integrand does not contain the singularity. When the distance between the observation and source points is not large, say $k|\mathbf{r} - \mathbf{r}'| < 5$, the integration over the mesh is performed numerically by using the Gauss-Legendre quadrature of the second order, otherwise the

integral is replaced by the integrand multiplied by the area of the mesh. To apply the Gauss-Legendre quadrature scheme to the integral over the quadrangle with vertices (u_1, v_1), (u_2, v_2), (u_3, v_3) and (u_4, v_4), the transformation of the variables (u, v) into (ξ, η) is made using the relations

$$\begin{pmatrix} u \\ v \end{pmatrix} = \frac{1}{4}(1-\xi)(1-\eta)\begin{pmatrix} u_1 \\ v_1 \end{pmatrix} + \frac{1}{4}(1+\xi)(1-\eta)\begin{pmatrix} u_2 \\ v_2 \end{pmatrix} + \frac{1}{4}(1-\xi)(1+\eta)\begin{pmatrix} u_3 \\ v_3 \end{pmatrix} + \frac{1}{4}(1+\xi)(1+\eta)\begin{pmatrix} u_4 \\ v_4 \end{pmatrix} \quad (4)$$

Then the quadrangle is changed to the square.

To verify the numerical code, the RCS patterns of $7\lambda \times 14\lambda$ cylinderical cavity of perfect conductor with a flat termination since the modal solution is available [4]. The agreement is quite well. The results converge roughly with N=3 iteration as pointed out in [2].

Fig. 4 shows the RCS patterns of the smaller $4\lambda \times 4\lambda$ cylindrical cavity. Both the case of the perfect conductour and impedance interior walls are considered. The results of perfect conductor walls are compared with those given in [2], and are found to agree well. The normalized surface impedance are chosen to be $\zeta_1 = 0.40 + j0.115$ and $\zeta_2 = 0.351 + j0.0862$. The reason of choosing the close values of impedances is to verify the program since it is expected that the both results give close patterns. The size of the mesh of [2] is $0.33\lambda \times 0.33\lambda$, but smaller and differet size $0.15\lambda \times .25\lambda$ is used here. The mesh size of [2] seems to be sufficient for practical computation. It was pointed in [2] that the number of iteration $N = 3$ is sufficient for perfectly conducting cavities, this criterion is found to hold also for the impedance cavity.

4. Conclusion

The radar cross section of the open-ended circular waveguide cavity with impedance interior walls was computed by using the iterative physical optics algorithm. It is verified that the impedance walls are effective for reduction of the RCS of the open-ended cavity. Since the shape of the mesh is a quadrangle, instead of square, the numerical code developed here can be readily applied to the cavities with more complex configuration.

References

[1] H. Ling, R.C Chou and S.W. Lee, Shooting and bouncing rays, calculating the RCS of an arbitrary shaped cavity, IEEE Trans. vol. AP-37, pp.194-205, 1989.

[2] F. Obelleiro-Basteiro, J. L. Rodriguez and R. J.Burkholder, An iterative physical optics approach for analysing the electromagnetic scattering by large open-ended cavities, IEEE Trans. vol. AP-43, pp.356-361, 1995.

[3] F. Obelleiro-Basteiro, J. L. Rodriguez and A. G. Pino, A progressive physical optics method for computing the electromagnetic scattering of large open-ended cavities, Microwave and Optics Tech. Letters, vol. 14, pp.166-169, 1997.

[3] D. B. Miron, The singular problem in surface, IEEE Trans. vol. AP-31, pp.507-509, 1983

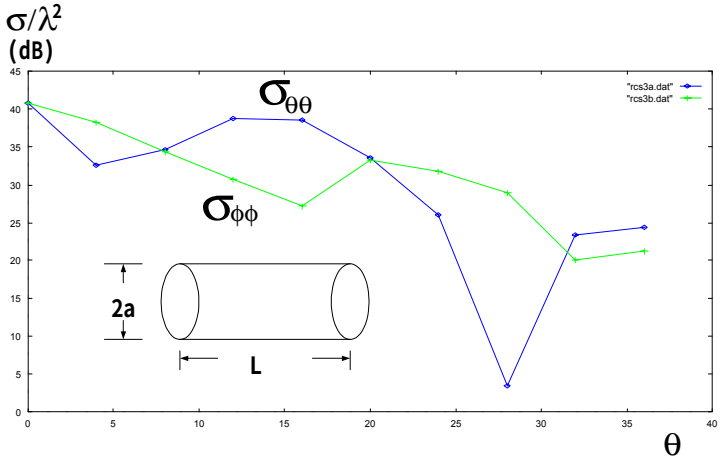

Fig.3 RCS of open-ended cavity of perfect conductor. $a = 3.5\lambda$, $L = 14\lambda$

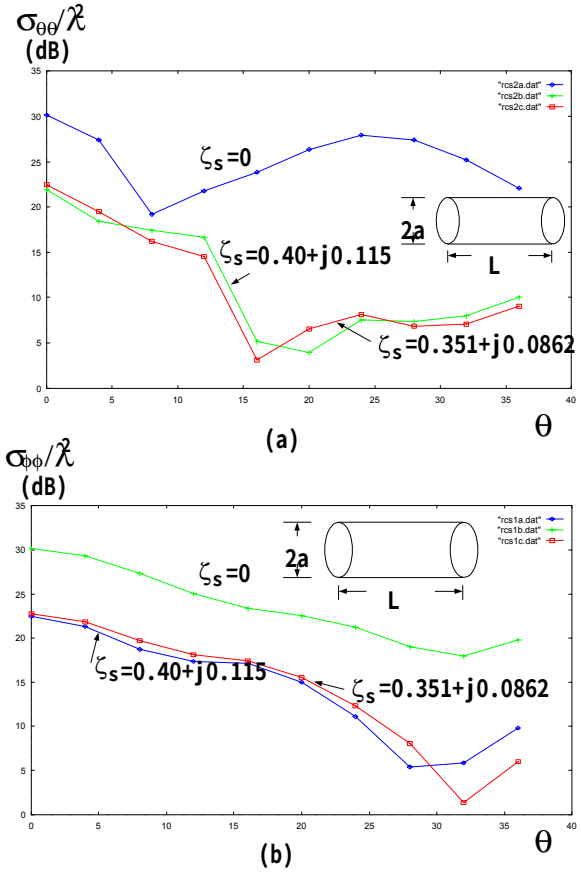

Fig.4 RCS of open-ended cavity with perfect conductor walls and surface impedance walls $a = 2\lambda$, $L = 4\lambda$. **(a):** $\sigma_{\theta\theta}$ **(b):** $\sigma_{\phi\phi}$